Accepted Manuscript

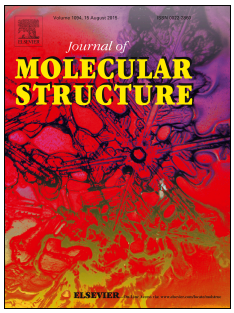

Structural, absorption, and molecular properties of o,o'-dihydroxyazo resorcinol dyes bearing an acryloyloxy group

Sevil Özkınalı, M. Serdar Çavuş, Abdullah Ceylan, Mahmut Gür

PII: S0022-2860(17)31043-8

DOI: 10.1016/j.molstruc.2017.07.099

Reference: MOLSTR 24126

To appear in: *Journal of Molecular Structure*

Received Date: 27 March 2017

Revised Date: 27 July 2017

Accepted Date: 28 July 2017

Please cite this article as: S. Özkınalı, M.S. Çavuş, A. Ceylan, M. Gür, Structural, absorption, and molecular properties of o,o'-dihydroxyazo resorcinol dyes bearing an acryloyloxy group, *Journal of Molecular Structure* (2017), doi: 10.1016/j.molstruc.2017.07.099.

Structural, Absorption, and Molecular Properties of o,o'-Dihydroxyazo Resorcinol Dyes Bearing an Acryloyloxy Group

Sevil Özkınalı[1]*, M. Serdar Çavuş[2], Abdullah Ceylan[1], Mahmut Gür[3]

[1]Department of Chemistry, Faculty of Science and Literature, Hitit University, Çorum, Turkey

[2]Biomedical Engineering Department, Faculty of Engineering and Architecture, Kastamonu University, Kastamonu, 37100, Turkey

[3]Department of Forest Industrial Engineering, Faculty of Forestry, Kastamonu University, Kastamonu, Turkey

*Corresponding Author.

Tel: +903642267000-1636;

Fax: +903642277005

e-mail: sevilozkinali@hitit.edu.tr

Abstract

To the best of our knowledge, this is the first study reporting the synthesis and characterization of *o,o′*-dihydroxyazo dyes bearing an acryloyl group. The *o,o′*-dihydroxyazo dyes were synthesized through coupling of resorcinol with the diazonium salts of 2-amino-4-methylphenol, 2-aminophenol, 2-amino-4-chlorophenol, and 2-amino-4-nitrophenol. Their acryloyl derivatives were synthesized using metallic sodium and acryloyl chloride under an inert atmosphere. Characterization of the compounds was conducted using infrared (IR), ultraviolet–visible (UV–Vis), proton nuclear magnetic resonance (^{1}H NMR), and carbon nuclear magnetic resonance (^{13}C NMR) spectroscopic methods. The tautomerism of the synthesized compounds' was also

evaluated. The results were compared with theoretical results obtained by density functional theory (DFT). The DFT calculations were performed to obtain ground-state optimized geometries and calculate the relevant electronic and chemical reactivity parameters. Furthermore, possible tautomers deduced from the UV–Vis spectra were investigated using theoretical calculations. Both the IR and NMR spectral data showed that azo tautomers predominate in the solid state and DMSO solvent. The effects of pH, solvent, and substituent on the predominant tautomers were further investigated through UV–Vis spectroscopy. The results indicate that hydrazone tautomers were dominant at pH 12 in dimethylformamide (DMF), whereas azo tautomers were dominant at pH 2 in EtOH or $CHCl_3$.

Keywords: *o,o′*-dihydroxyazo dyes, DFT, azo–hydrazone, tautomerism, resorcinol

Graphical Abstract

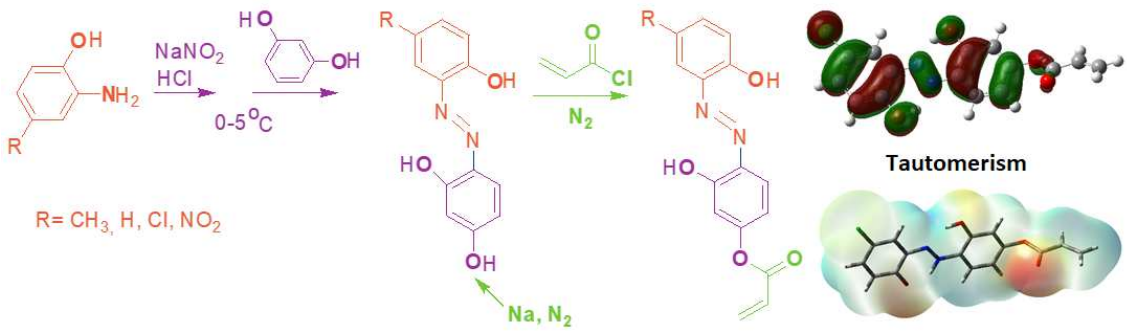

Highlights

- Novel *o,o*'-dihydroxyazo dyes containing an acryloyl moiety were synthesized and characterized.
- The azo–hydrazone tautomerism was investigated using UV–Vis spectroscopy and DFT calculations.
- These compounds are useful for synthesizing novel organic dyes.

1. Introduction

Azo dyes have been extensively used in various fields such as textiles, paper, leather, gasoline, food, additives, cosmetics, analytical chemistry, photography, therapeutic agents, and drug delivery [1–5]. Such dyes are pertinent to photography, xerography, laser printing, and write once-read many times memory systems due to their fastness properties, low production costs, and useful applications [1,6,7]. Azo dyes are also pertinent to the medical and pharmaceutical industries owing to their antiseptic, antibacterial, antitumor, antioxidant, antineoplastic, and antidiabetic properties [2,8,9]. In particular, azo resorcinol dyes have been studied for their significant antioxidant and antimicrobial activities [10]. Resistance of bacteria to modern antibiotics has recently become a clinical crisis. Medicinal chemists are developing new antibiotics and synthetic antimicrobial agents to conquer drug-resistant strains [10]. For example, 4-*n*-butyl resorcinol has been used in skin creams and lotions due to its antimicrobial and bleaching action efficacy [11,12]. Moreover, due to their phenolic moiety and hydroxyl groups, azo resorcinol dyes are commonly used as colorimetric reagents for metal ions [13–15].

Azo–hydrazone tautomerism occurs within azo compounds bearing, at a minimum, a protic group in conjugation with the azo groups [16]. In particular, *o*,*o'*-dihydroxyazo dyes can exhibit azo–hydrazone tautomerism. The tautomeric equilibrium primarily depends on structural factors, solvent polarity, and pH of the medium [17–18]. Kishimoto et al. [19] demonstrated that the azo group (-N=N-) is an electron-accepting group; thus, electron-donating groups stabilize the azo tautomer. Hydrazones bearing electron-acceptor groups such as imino (-NH-N=) are stabilized via electron-donor groups. [19]. Dakiky et al. [20] noted solvent effects on tautomerism. High-polarity

solvents favor hydrazone tautomers, whereas low-polarity solvents prefer azo tautomers [20]. Pertinent to tautomeric characterization is the fact that the absorption bands of hydrazo tautomers are at longer wavelengths relative to the corresponding azo tautomers [21]. Azo dye tautomerism is pertinent to optical, technical, and environmental applications [22–23]. Numerous recent studies have investigated the molecular properties of azo dyes using density functional theory (DFT) calculations [24–30].

The aim of this study was to analyze the tautomers of eight novel azo resorcinol compounds that belong to the class of *o,o′*-dihydroxyazo dyes. The compounds were characterized using spectroscopy and DFT calculations to further understand azo–hydrazone tautomerism. The experimental results were validated using theoretical calculations. Although resorcinol dye synthesis and spectroscopic properties have been previously reported, no study has examined *o,o′*-dihydroxyazo resorcinol dyes bearing an acryloyl moiety nor have they implemented DFT [12,20]. DFT calculations illustrate the extent to which experimental results match theoretical predictions.

The azo derivatives reported herein were characterized by IR, UV–Vis, ^{1}H NMR, and ^{13}C NMR spectroscopies. DFT calculations with different basis sets were used to evaluate the structural and chemical properties of the compounds. Tautomerization was examined using experimental and theoretical UV–Vis studies. The molecular geometry, optimized parameters, and UV–Vis absorption values were calculated, and the calculated spectral data were compared with the experimental results.

2. Experimental

Chemicals and solvents were purchased from Aldrich (USA) and Merck Chemical Company (Germany) and used without further purification. The IR spectra were obtained using a Thermo Scientific Class 1 Laser Product FTIR (USA) spectrophotometer in the ATR mode. The absorption spectra in chloroform, ethanol, and DMF were obtained using a Thermo Scientific Genesys 10S UV–VIS (UK) spectrophotometer. Elemental, ^{1}H NMR, and ^{13}C NMR analyses were conducted in the Instrumental Analysis Laboratory at METU Research Center. Nuclear magnetic resonance spectra were obtained on a Bruker (Germany) AC 400 Fourier Transform Spectrometer operating at 400 MHz in deuterated dimethylsulfoxide (DMSO-d_6) using tetramethylsilane (TMS). Substance purity and reaction progress were monitored by TLC using TLC aluminum sheets with silica gel 60 F254 (Merck). Preparative TLC chromatography was performed on 20 × 20 cm glass plates covered by silica gel 60 GF254 (Merck) or Al_2O_3 type G (Fluka (Switzerland)). Column chromatography was performed using silica gel 60 (Merck).

2.1. General procedure for the synthesis of acryloyl derivatives of azo dyes

First, *o,o'*-dihydroxyazo dyes were synthesized via a coupling reaction of resorcinol with diazonium salts of 2-hydroxy-4-methyl phenol, 2-aminophenol, 2-amino-4-choloro phenol, and 2-amino-4-nitro phenol [31–32]. Then, for the synthesis of acryloyl derivatives of *o,o'*-dihydroxyazo dyes, reaction of these compounds with metallic sodium and acryloyl chloride was conducted under a N_2 atmosphere at a 1:1 molar ratio. Figure 1 illustrates the general synthesis method and the structures of compounds **1**–**8**.

2.1.1. Synthesis of 4-[(*E*)-(2-hydroxy-5-methylphenyl)diazenyl]benzene-1,3-diol, (1)

A cold solution of $NaNO_2$ (0.69 g; 0.01 mol) was added dropwise into a mixture of 2-amino-4-methylphenol (1.23 g; 0.01 mol) dissolved in concentrated hydrochloric acid and water (20 mL) at 0–5°C. The solution was then stirred for 30 min to complete the diazotation. Diazonium salt was added dropwise into an ice-cold solution of 1,3-benzenediol (1.10 g; 0.01 mol) with a mixture of NaAc (7.5 g, 0.09 mol) and DMF (20 mL) at 0–5°C. After stirring for 3 h at 0–5°C, the solution acidity was adjusted to pH 4–5 using 1 $mol.L^{-1}$ HCl. The synthesized compounds were precipitated by maintaining a temperature range of 0–5°C. The reaction solution was then filtered and washed with water and purified from ethanol/water. Melting Point (m.p.) 153-155 °C. Yield 78 %. IR (cm^{-1}): 3277 (OH), 3067, 2976, 2916 (C-H), 1621 (>C=C<), 1178 (Ar-O) ^{1}H NMR (500 MHz, d_6-DMSO, ppm): 12.81 (s,1H), 11.08 (s,1H), 10.47 (s, 1H), 7.68 (d, 1H, *J* =7.00), 7.55 (s, 1H), 7.12 (d, 1H, *J*=5.50 Hz), 6.92 (d, 1H, *J*=7.0 Hz), 6.47 (d, 1H, *J*=5.50 Hz), 6.37 (s, 1H), 2.27 (s, 3H) ^{13}C NMR (125 MHz, d_6-DMSO, ppm) 162.9, 157.3, 151.4, 137.03, 132.7, 132.4, 128.9, 128.5, 121.4, 117.8, 109.4, 103.5, 20.5. Analysis by calculation for $C_{13}H_{12}N_2O_3$: C, 63.93; H, 4.95; N, 11.47 %. Found: C, 62.25; H, 5.14; N, 10.84%

2.1.2. Synthesis of 4-[(*E*)-(2-hydroxyphenyl)diazenyl]benzene-1,3-diol, (2)

The same procedure was used for the synthesis of compound **1** and compound **2**. The product was recrystallized from ethanol/water, yielding a product with a melting point (m.p.) in the range of 136–138°C. Yield 78 %. IR (cm^{-1}): 3488, 3199 (OH), 3095 (C-H), 1623 (>C=C<), 1167 (Ar-O) ^{1}H NMR (500 MHz, d_6-DMSO, ppm): 12.68 (s,1H), 11.42 (s,1H), 10.49 (s, 1H), 7.74 (d, 1H, *J* =5.50), 7.69 (d, 1H, *J*=6.50 Hz), 7.30 (t, 1H, *J*=5.50 Hz), 7.03 (d, 1H, *J*=7.0 Hz), 6.96 (t, 1H, *J*=6.50 Hz), 6.48 (d, 1H, *J*= 7.0 Hz), 6.38 (s, 1H) ^{13}C NMR (125 MHz, d_6-DMSO, ppm) 163.1, 157.4, 153.5, 137.5, 132.4,

131.9, 128.0, 122.1, 120.1, 118.0, 109.5, 103.5 Analysis by calculation for $C_{12}H_{10}N_2O_3$: C, 62.60; H, 4.38; N, 12.17 %. Found: C, 61.32; H, 4.53; N, 10.54%

2.1.3. Synthesis of 4-[(*E*)-(5-chloro-2-hydroxyphenyl)diazenyl]benzene-1,3-diol, (3)

The same procedure was used for the synthesis of compound **1** and compound **3.** The product was recrystallized from ethanol/water to give an orange dye with a m.p. in the range of 190–192°C. Yield 78 %. IR (cm^{-1}): 3447, 3184 (OH), 3080 (C-H), 1627 (>C=C<), 1169 (Ar-O), 980 (C-Cl) ^{1}H NMR (500 MHz, d_6-DMSO, ppm): 12.65 (s,1H), 11.18 (s,1H), 10.61 (s, 1H), 7.75 (s, 1H), 7.72 (d, 1H, *J*=7.50 Hz), 7.31 (d, 1H, *J*=8.20 Hz), 7.05 (d, 1H, *J*= 7.50 Hz), 6.49 (d,1H, *J*=8.20 Hz), 6,37 (s, 1H) ^{13}C NMR (125 MHz, d_6-DMSO, ppm) 163.8, 157.8, 152.7, 138.3, 132.8, 131.1, 129.0, 124.1, 119.6, 119.3, 109.9, 103.6. Analysis by calculation for $C_{12}H_9ClN_2O_3$: C, 54.46; H, 3.43; N, 10.58 %. Found: C, 53.25; H, 3.59; N, 10.14%

2.1.4. Synthesis of 4-[(*E*)-(2-hydroxy-5-nitrophenyl)diazenyl]benzene-1,3-diol, (4)

The same procedure was used for the synthesis of compound **1** and compound **4**. The product was recrystallized from ethanol/water to give a red dye, yielding a product with a m.p. in the range of 152–156°C. Yield 72 %. IR (cm-1): 3492, 3404 (-OH), 3093 (C-H), 1621 (>C=C<), 1516,1338 (NO_2), 1182 (Ar-O) ^{1}H NMR (500 MHz, d_6-DMSO, ppm): 12.79 (s,1H), 12.36 (s,1H), 10.77 (s, 1H), 8.49 (s, 1H), 8.15 (d, 1H, J=5.00 Hz), 7.76 (d, 1H, J=7.50 Hz), 7.21 (d, 1H, J= 7.50 Hz), 6.51 (d,1H, J=5.00 Hz), 6,38 (s, 1H) ^{13}C NMR (125 MHz, d_6-DMSO, ppm) 164.4, 159.6, 158.3, 140.6, 137.0, 132.9, 129.5, 126.4, 118.4, 114.9, 110.2, 103.4 Analysis by calculation for $C_{12}H_9N_3O_5$: C, 52.37; H, 3.30; N, 15.27 %. Found: C, 53.08; H, 3.73; N, 15.46%

2.1.5. Synthesis of 3-hydroxy-4-[(*E*)-(2-hydroxy-5-methylphenyl)diazenyl]phenyl prop-2-enoat, (5)

4-[(*E*)-(2-Hydroxy-5-methylphenyl)diazenyl]benzene-1,3-diol (549.0 mg; 2.25 mmol) and fresh metallic sodium (51.74 mg; 2.25 mmol) in dry THF (20 mL) were mixed and stirred under a N_2 atmosphere for 24 h. Then, acryloyl chloride (0.189 mL; 2.25 mmol) was added dropwise and stirred into a mixture under a dry nitrogen atmosphere. After stirring for 4 h, the reaction mixture was filtered and the desired product was precipitated from the dried THF. The final product was recrystallized from THF/water, yielding a product with a m.p. in the range of 116–118°C. Yield 58 %. IR (cm^{-1}): 3198 (OH), 3072, 2922 (C-H), 1742 (C=O), 1624, 1601 (>C=C<), 1240, 1160 (Ar-O) ^{1}H NMR (500 MHz, d_6-DMSO, ppm): 12.84 (s, 1H) 11.09 (s, 1H), 7.67 (d, 1H, *J*=7.0), 7.54 (s, 1H), 7.35-7.16 (m, 1H), 7.10 (d, 1H, *J*=5.50), 6.92 (d,1H, *J*=7.0), 6.58-6.50 (m,1H), 6.48 (d, 1H, *J*=5.50), 6.33 (s, 1H), 6.22-6.17 (m, 1H), 2.27 (s, 3H) ^{13}C NMR (125 MHz, d_6-DMSO, ppm) 164.6, 155.4, 153.8, 152.5, 138.3, 134.7, 134.5, 129.2, 128.5, 127.9, 124.9, 123.7, 118.7, 114.1, 111.4, 21.0 Analysis by calculation for $C_{16}H_{14}N_2O_4$: C, 64.42; H, 4.73; N, 9.39 %. Found: C, 63.79; H, 4.48; N, 9.49%

2.1.6. Synthesis of 3-hydroxy-4-[(*E*)-(2-hydroxyphenyl)diazenyl]phenyl prop-2-enoat, (6)

The same procedure was used for the synthesis of compound **5** and compound **6.** The product was then recrystallized from THF/water, yielding a product with a m.p. in the range of 113–115°C. Yield 72 %. IR (cm^{-1}): 3202 (OH), 3064, 2922, 2853 (C-H), 1740 (C=O), 1615, 1581 (>C=C<), 1241, 1125 (Ar-O) ^{1}H NMR (500 MHz, d_6-DMSO, ppm): 12.80 (s, 1H) 11.46 (s, 1H), 7.88 (d, 1H, J=7.5), 7.73 (d, 1H, J=6.5), 7.67 (d, 1H, J=7.5), 7.29 (t, 1H, J=6.5), 7.06 (d, 1H, J=4.0), 6.95 (t, 1H, J=6.5), 6.87-6.85 (m, 1H), 6.49 (d,

1H, J= 4.0), 6.37 (s,1H), 6.22-6.15 (m, 1H) ^{13}C NMR (125 MHz, d_6-DMSO, ppm) 164.5, 162.3, 155.4, 154.3, 138.7, 137.8, 136.0, 132.1, 128.1, 121.8, 120.3, 118.9, 118.8, 109.6, 103.6 Analysis by calculation for $C_{15}H_{12}N_2O_4$: C, 63.38; H, 4.25; N, 9.85 %. Found: C, 63.06; H, 4.08; N, 9.13%

2.1.7. Synthesis of 3-hydroxy-4-[(*E*)-(5-chloro-2-hydroxyphenyl)diazenyl]phenyl prop-2-enoat, (7)

The same procedure was used for the synthesis of compound **5** and compound **7.** The product was then recrystallized from THF/water, yielding a product with a m.p. in the range of 180–182°C. Yield 54 %. IR (cm^{-1}): 3082 (-OH), 2970, 2852 (C-H), 1746 (>C=O), 1622, 1595 (>C=C<), 1256, 1158 (Ar-O), 979 (C-Cl) ^{1}H NMR (500 MHz, d_6-DMSO, ppm): 12.65 (s, 1H) 11.18 (s, 1H), 7.75 (s, 1H), 7.71 (d, 1H, J=10.0), 7.58-7.40 (m, 1H), 7.31 (d, 1H, J=10.0), 7.06 (d, 1H, J=10.0), 6.93 (d, 1H, J=10.0), 6.60-6.45 (m, 1H), 6.37 (s, 1H), 6.25-6.16 (m, 1H) ^{13}C NMR (125 MHz, d_6-DMSO, ppm) 164.4, 157.3, 152.2, 145.5, 143.2, 137.8, 134.6, 131.5, 127.4, 126.8, 123.6, 118.7, 116.7, 109.3, 102.9 Analysis by calculation for $C_{15}H_{11}ClN_2O_4$: C, 56.53; H, 3.48; N, 8.79 %. Found: C, 56.26; H, 3.40; N, 8.76%

2.1.8. Synthesis of 3-hydroxy-4-[(*E*)-(2-hydroxy-5-nitrophenyl)diazenyl]phenyl prop-2-enoat, (8)

The same procedure was used for the synthesis of compound **2** and compound **8**. The product was then recrystallized from THF/water, yielding a product with a m.p. in the range of 116–118°C. Yield 62 %. IR (cm^{-1}): 3178 (-OH), 3100, 2918, 2853 (C-H), 1749 (C=O), 1623, 1578 (>C=C<), 1527, 1343 (NO_2), 1211, 1112 (Ar-O)) ^{1}H NMR (500 MHz, d_6-DMSO, ppm): 13.15 (s, 1H) 11.98 (s, 1H), 8.70 (s, 1H), 8.15-8.12 (m, 1H),

7.95 (d, 1H, *J*=7.50), 7.78-7.71 (m, 1H), 7.60 (d, 1H, *J*=7.50), 6.98-6.78 (m, 1H), 6.57-6.48 (m,1H), 6.30 (s, 1H), 6.13-6.07 (m, 1H) ^{13}C NMR (125 MHz, d_6-DMSO, ppm) 164.9, 159.0, 157.8, 150.9, 146.1, 142.7, 135.1, 133.3, 127.3, 124.9, 117.9, 114.5, 112.0, 109.7, 102.9. Analysis by calculation for $C_{15}H_{11}N_2O_6$: C, 54.72; H, 3.37; N, 12.76 %. Found: C, 54.42; H, 3.40; N, 12.05%

2.2. Computational Methods

Structural optimization of compounds was performed by DFT calculations using suitable basis sets without any geometric constraints. The Kohn–Sham density functional theory [33–34] was used to calculate the compounds' ground-state geometries and excitation energies. Molecular structures of the compounds in the ground state were optimized using the M06 method (which is a set of four meta-hybrid GGA DFT functionals) with 3-21G basis set; the B3LYP method (*Becke3–Lee–Yang–Parr hybrid functional*) with 6-311++G and 6-311++G(2d,2p) basis sets; and the PBE1PBE method (which is the generalized-gradient-approximation exchange–correlation functional of Perdew, Burke, and Ernzerhof) with cc–pvtz basis set in chloroform, dimethylformamide, and ethanol solvents.

In order to determine the minimum energy level configuration of the compounds, compound **1** was dihedrally scanned around the N=N bond with a step size of 18° for a total of 20 steps (Figure 2). The most suitable dihedral angle that gives the minimum energy level of the compound between the phenyl rings was calculated as 7.74°. Calculations for geometric optimization of the remaining compounds followed the aforementioned protocol. In the calculations, the compounds' minimum molecular

energies were obtained by the level 6-311++G(2d,2p) basis set using the B3LYP method. The optimized geometries were used in UV–Vis-based molecular calculations. The self-consistent reaction field (SCRF) method and the conductor-polarizable continuum model (CPCM) were used for such calculations. The frontier molecular orbitals (FMOs) energies were also calculated as per the same methods and basis sets. FMO energy eigenvalues were used to calculate global chemical reactivity parameters such as chemical hardness, chemical softness, and electronegativity. Dipole moment and molecular electrostatic potential (MEP) surfaces of the optimized molecular structures were examined using the theoretical results. All calculations in the study were performed using the GAUSSIAN 09 software package program [35].

3. Results and Discussion

3.1. Synthesis

Figure 1 shows the synthetic route toward the azo dyes and previously unreported acryloyl derivatives. All the compounds were synthesized as described previously [36]. Aromatic amines were effectively diazotized at 0–5°C using sodium nitrite and hydrochloric acid. Esters were derived satisfactorily by adding acryloyl chloride to the sodium salts of the resorcinol dyes in an inert atmosphere, and purification was performed in EtOH. Dye purity was verified using TLC with a chloroform:methanol (4:1) solvent system. Azo dyes and their acryloyl derivatives were identified through IR, UV–Vis, ^{1}H NMR, and ^{13}C NMR spectroscopies.

3.2. IR spectral analysis

Two hydroxyl peaks were determined in the IR spectra of the resorcinol dyes. The first peak was at 3387–3095 cm^{-1} for the compounds containing an intramolecular hydrogen bond between the phenolic and azo groups. The second and narrow peak was observed at 3540–3489 cm^{-1}, attributable to free hydroxyl groups. The absorption band corresponding to the free hydroxyl group was not observed in the IR spectra of the acryloyl derivatives. These observations indicate a successful reaction. On comparing the spectra of the azo dyes and their acryloyl derivatives, strong carbonyl peaks were observed in the 1740–1749 cm^{-1} range (Table 1 and Fig. 3). The peaks between 2970 and 2852 cm^{-1} were assigned to the –C-H stretching frequency of the ethenyl (–$CH=CH_2$) moiety of the acryloyl derivatives. The remaining stretching bands at 1623–1578 cm^{-1}, 1279–1236 cm^{-1}, and 1167–1110 cm^{-1} were attributed to ethenyl (CH_2=CH-), aromatic (-C=C-), -C(O)-O- and Ar-O-, respectively. After acryloyl derivative esterification, the stretching frequencies of the–C(O)-O- group appeared as a broader and stronger peak with Ar-O stretches in the same region. An–NH peak originating from hydrazone enantiomers, which would appear in the same region of the hydroxyl peak, was not observed. Azo–hydrazone tautomerization occurs via proton transfer from the hydroxyl group to the azo group. In the literature, NH peaks are seen in the vicinity of 3109 cm^{-1} as a weak peak [37]. Therefore, the absence of –NH peaks indicates that the compounds are azo tautomers in solid state.

3.3. UV–Vis spectral analysis

UV–Vis spectral data were recorded in various solvents such as $CHCl_3$, EtOH, and DMF. The effect of pH on the absorption spectra of compounds (**1–8**) was investigated in DMF by adjusting the pH to 2 and 12 using 0.1 $mol.L^{-1}$ HCl and 0.1 $mol.L^{-1}$ NaOH. Table 2 shows the UV–Vis absorption bands pertinent to compounds **1**–**8**.

The absorption maxima (λ_{max}) for compounds **1**–**8** were measured in ethanol as 395–403 nm and 415–469 nm, in chloroform as 335–401 nm and 423–436 nm, in DMF as 392–428 nm and 435–529 nm, in DMF at pH 2 as 396–431 nm and 441–511 nm, and in DMF at pH 12 as 360–450 nm and 495–510 nm. This indicates a high molar absorptivity attributable to the $\pi \rightarrow \pi^*$ and $n \rightarrow \pi^*$ transitions. Figure 4 shows the UV–Vis spectrum of compound **7**. These results are elaborated and explained next.

The λ_{max} of the dyes and their acryloyl derivatives in DMF with pH 12 showed a slightly bathochromic shift compared with EtOH and $CHCl_3$. Azo dye **1**, bearing an electron-donor substituent exhibited a bathochromic shift in EtOH. In contrast, azo compounds **3** and **4**, bearing electron-acceptor substituents, exhibited a hypsochromic shift compared with unsubstituted azo compound **2**. Resorcinol azo dyes **1**–**4** featured a hypsochromic shift compared to the corresponding acryloyl derivatives (**5**–**8**) in all solvents because of the electron-withdrawing effect of the acryloyl group. As a result of the observed bathochromic shifts, pH 12 DMF favors the hydrazone tautomers. Theoretical predictions of the hydrazone tautomers **A**–**E** of compounds **1–8** were undertaken to analyze in detail the tautomeric equilibrium observed in the experimental UV–Vis data (Figure 5 and Section 3.5).

3.4. NMR spectral analysis

^1H NMR and ^{13}C NMR chemical shifts were recorded in d_6-DMSO. In the ^1H NMR spectra of the azo dyes, peaks of three hydroxyl groups were observed as a singlet peak at 12.81–12.65 ppm, 12.36–11.08 ppm, and 10.90–10.47 ppm. The protons of the two hydroxyl groups in the esterified products were determined between 11.95 and 11.08 ppm (and in the case of hydrogen bonding, from 10.90 to 10.47 ppm). The third peak,

which resonated in the range of 12.81–12.65 ppm, disappeared as expected after esterification. In Dyes **1** and **5**, which bear a methyl group on the diazo unit, methyl protons resonated as a singlet peak at 2.27 ppm. The peaks between 8.70 and 6.07 ppm were attributed to the signals of aromatic and vinyl protons (Table 3 and Fig. 6). The ^{13}C NMR spectra of acryloyl derivatives showed a low field signal at 164 ppm, which can be attributed to the carbon atom of the >C=O group. Compounds **1**–**4** may be expected to favor the azo tautomer in DMSO solvent since the carbonyl groups expected for the hydrazone tautomer were not detected. The vinyl peaks of the acryloyl derivatives resonated in the range of 162.3–102.9 ppm, close to the aromatic carbon atom region (Table 4). The peaks appearing at 21 ppm of compounds **1** and **5** are attributed to the carbon atom of the methyl group. The NMR data obtained in this study are consistent with the literature [38].

3.5. Theoretical Results

The results of the B3LYP method with the 6-311 ++ G (2d, 2p) basis set were used in this study due to experimental pertinence. The Appendix (supplementary data) shows the data obtained from other methods and basis sets. The experimental UV–Vis absorptions obtained in chloroform and ethanol compare favorably with theoretical calculations. The absorption wavelengths of compounds **1**–**8** were calculated to be between 411 nm and 443 nm in chloroform and between 411 nm and 431 nm in ethanol (Table 5).

The UV–Vis theoretical calculations indicate that the bonding of the acryloyl group to the resorcinol derivatives caused shifts to longer wavelengths. Considering the resorcinol derivatives, the absorption wavelengths of the CH_3, Cl, and NO_2 substituents

on the *m*-position of the phenyl ring are as follows: $\lambda_{max(\mathbf{1})} > \lambda_{max(\mathbf{5})} > \lambda_{max(\mathbf{7})}$. Thus, the *m*-$CH_3$ leads to an enhanced bathochromic shift in comparison to *m*-Cl and *m*-NO_2. This λ_{max} trend is the same for CH_3, Cl, and NO_2 derivatives of acryloyl compounds **5**, **7**, and **8**.

The absorption maxima in DMF shifted to longer wavelengths in the experimental studies than that in chloroform and ethanol. Experimental UV studies showed that all compounds absorbed in the 495–510 nm range at pH = 12 and in the 490–529 nm range in DMF (not pH-adjusted). These shifts can be ascribed to the conversion of the azo compounds and their acryloyl derivatives to hydrazone tautomers, as a function of solvent and acidity. However, it is difficult to evaluate tautomerization through experimental UV–Vis spectra. In order to clarify this interpretation, theoretical calculations were performed with the B3LYP method with 6-311++G(2d,2p) basis set for all possible hydrazone tautomeric structures in DMF. Figure 6 shows the possible tautomers. Theoretical results obtained for hydrazones **C** and **E** are most pertinent to the experimental results (Table 6). The calculated UV absorption values for the tautomers were obtained in the range of 486–513 nm for B3LYP/bs3. Both the experimental and theoretical results showed that the UV–Vis absorptions of the resorcinol derivative, considering the possible tautomers, manifest at shorter wavelengths than their acryloyl derivatives.

The molecular energy of compounds **1**–**8** obtained using the B3LYP method with 6-311++G(2d,2p) was calculated to be lower than that of the other methods and basis sets. In the calculations, the minimum molecular energies of the resorcinol derivative compounds were calculated to be as follows: –1.258.324 au for *m*-Cl (molecule **3**), –1.003.271 au for *m*-NO_2 (molecule **4**), –838.030 au for *m*-CH_3 (molecule **1**), and –

798.701 au for the unsubstituted derivative (compound **2**). A similar sequence of energy values was also observed for acryloyl derivatives **7**, **8**, **5**, and **6**. Furthermore, the *m*-NO_2 substituted compounds **4** and **8** have a much larger dipole moment than the other compounds. In comparison, *m*-Cl substituted compounds **3** and **7** have a larger dipole moment than the remaining compounds (**1**, **2**, **5**, and **6**). Therefore, bonding of the acryloyl group to the resorcinol derivatives caused a decrease in the energy gap ($\Delta E = E_{LUMO} - E_{HOMO}$) and molecular hardness but caused an increase in electronegativity. The highest ΔE and chemical hardness (η) values were observed for *m*-NO_2 substituted compounds **4** and **8** (Table 7). Appendix 1–3 provides additional data.

Calculations for the azo–hydrazone tautomers provided remarkable results. The molecular energies of the hydrazones should be lower than those of the azo compounds. It is obvious that theoretical calculations gave results that support this expectation (Table 8). However, the relationship between the calculated minimum molecular energy levels of possible tautomers may not be the only indication of which tautomers are present over the course of the experiment. Theoretical calculations indicate that the compound with the lowest molecular energy for the azo–hydrazo compounds is the possible hydroazo tautomer **A**, and the proposed tautomeric structure **D** for acryloyl group molecules has lower molecular energies than those of the remaining possible structures (Appendix 4). However, when the calculated energy gap (ΔE) of possible tautomers is examined, one encounters an interesting result: within the proposed tautomeric structures, the energy gap of **C** and **E**, which compare favorably with the experiments, is markedly smaller than that of other possible situations. Similarly, the chemical hardness values of compounds **C** and **E** are also calculated to be quite small compared to other possible situations.

Tautomerization affected LUMO energies more than HOMO energies, and consequently the difference between the HOMO–LUMO energies decreased (Figure 7 for compounds **1** and **5**; Appendices 5a and 5b show other HOMO–LUMO and ESP maps of the azo–hydrazone tautomers). The chemical hardness for the ground state of an N electronic system is defined as

$$\eta = \frac{1}{2}\left(\frac{\partial^2 E}{\partial N^2}\right)_{V(\vec{r})}, \quad (1)$$

where E is the electronic energy, N is the number of electrons, and $V(\vec{r})$ is the constant external potential. Equation 1 can be expressed using the finite difference approximation

$$\eta = \frac{1}{2}(I - A), \quad (2)$$

where I and A can be approximated in terms of the energies of the FMOs; i.e., $I = -E_{\mathrm{HOMO}}$ and $A = -E_{\mathrm{LUMO}}$ [39]. From Equations 1 and 2, the hydrazone tautomers are more likely to be chemically reactive than the azo tautomers. In other words, hydrazones are chemically softer than azo tautomers.

In addition, a noticeable increase in dipole moments of the hydrazone tautomers was observed. In particular, the dipole moments of compounds **4** and **8** bearing *m*-NO_2 were higher than those of other molecules. An interesting situation pertains to the correlation between the energy gap of possible hydrazone and azo tautomers. The Pearson correlation coefficient R of the relationship between the energy gaps of hydrazones **C** and **E** and the azo tautomers of compounds **1**–**8** was calculated to be 0.4988. For a combination of hydrazones **A**, **B**, and **D**, the correlation coefficients were calculated to be 0.7809 for **A**–**D** and 0.8209 for **B**, **D** (Graphic 1).

The HOMO–LUMO energies of hydrazones **C** and **E**, which compare more favorably with the experimental UV–Vis values, changed in a less-correlated fashion than those of the other hydrazones. In other words, if there is a higher correlation between the hydrazone and azo tautomers, the molecular electronic configurations of the compounds are more protected; i.e., more resistant to a configurational change. Therefore, these structures contribute less to the tautomerism.

4. Conclusion

In this research, *o,o′*-dihydroxy azo dyes that bear an acryloyl moiety were synthesized through a reaction between *o,o′*-dihydroxy azo dyes and acryloyl chloride in a 1:1 molar ratio. The structures of these compounds were characterized using IR, UV–Vis, ^{1}H NMR, and ^{13}C NMR. In the UV–Vis spectra, the absorptions of compounds **1-8** in DMF revealed significant shifts in acidic and basic conditions compared with neutral pH and other solvents. After esterification, free hydroxyl peaks did not appear in the IR spectra as expected. In the ^{13}C NMR spectra of the acryloyl compounds in d_6-DMSO, a carbonyl peak was observed in the vicinity of 164 ppm. Both IR and NMR spectroscopies showed that azo tautomers of azo and acryloyl derivatives were dominant in the solid state and DMSO solvent.

The tautomerism proposed from experimental UV–Vis data was studied in detail by quantum chemical calculations. Consequently, the Pearson correlation and energy gap, ΔE, was useful to determine the dominant tautomers. Although the energy gaps of structures **C** and **E** were smaller than other hydrazones, the Pearson correlation coefficient (R) of the relationship between structures **C** and **E** and the azo structures was

lower than that of other correlations. The chemical hardness of hydrazones **C** and **E** was calculated to be lower than that of other hydrazones. To the best of our knowledge, this report is the first example of *o,o'*-dihydroxy resorcinol azo dyes bearing an acryloyl moiety.

Acknowledgement

This study was supported by Scientific Research Council of Hitit University (Project No: FEF 19001.14.005).

References

[1] A. Hassanzadeh, A. Zeini-Isffahani, M.H. Habibi, M.R.A. Poor Heravi, M. Abdollahi-Alibeik, ^{1}H, ^{13}C, N-H, H-H, C-H COSY, H-H NOESY NMR and Uv-Vis studies of Solophenyl red 3BL dye azo-hydrazone tautomerism in various solvents. Spectrochimica Acta Part A. 63 (2006) 247-254.

[2] C. J. Patil, C. A. Nehete, The azo derivatives of salicylic acid, International Journal of Pharmaceutical Sciences Review and Research 33(2) (2015) 248-256.

[3] C. T. K. Kumara, J. Keshavayya, T. Rajesh, S. K. Peethambarb, R. A. S. Alı, Synthesis, characterization and antimicrobial activity of heterocyclic azodyes derived from thiadiazole, Chemical Science Transactions 2(4) (2013) 1346-1351.

[4] P. Patel, D. Gor, P. S. Patel, Design, synthesis and pharmacological evaluation of new series of pyrazolines based thiazolidin-4-one derivatives, Chemical Science Transactions 2(4) (2013) 1089-1093.

[5] S. Shahab, F. H. Hajikolaee, L. Filippovich, M. Darroudi, V. A. Loiko, R. Kumar, M. Y. Borzehandani, Molecular structure and UV-Vis spectral analysis of new synthesized azo dyes for application in polarizing films, Dyes and Pigments 129 (2016) 9-17.

[6] H. Valizadeh, A. Shomali, J. Ghorbani, S. Noorshargh, Synthesis of a nitrite functionalized star-like poly ionic compound as a highly efficient nitrosonium source and catalyst for the diazotization of anilines and subsequent facile synthesis of azo dyes under solvent-free conditions, Dyes and Pigments 117 (2015) 64-71.

[7] M. Özkütük, E. İpek, B. Aydıner, S. Mamaş¸ Z. Seferoğlu, Synthesis, spectroscopic, thermal and electrochemical studies on thiazolyl azo based disperse dyes bearing coumarin, Journal of Molecular Structure 1108 (2016) 521-532.

[8] H. G. Garg, C. Prakash, Preparation of 4-arylazo-3,5-disubstituted-(2H)-1,2,6-thiadiazine 1,1-dioxides, Journal of Medicinal Chemistry 15(4) (1972) 435-436.

[9] A. H. Shridhar, J. Keshavayya, S. K. Peethambar, H. Joy Hoskeri, Synthesıs of 1,3,4-oxadıazole incorporated azo dye derivatives as a potent biological activity molecules, International Journal of Pharmacy and Pharmaceutical Sciences 4 (12) (2012) 386-390.

[10] D. K. Sureja, K. R. Vadalia, $POCl_3$ catalyzed, one-step, solvent-free synthesis of some novel thieno[2,3-d]pyrimidin-4(3H)-one derivatives as antimicrobial agent, Journal of Saudi Chemical Society http://dx.doi.org/10.1016/j.jscs.2016.07.004

[11] S. K. Paidesetty, S. K. Rout, J. Sahoo, Antimicrobial and antioxidant activities of some newly synthesized benzene-1, 3-diol congeners and their characterization, International Journal of Pharmacy and Pharmaceutical Sciences 7 (7) (2015) 427-433.

[12] I. H. Pandya, R. N. Jadeja, K. J. Ganatra, Spectral characterization and biological evaluation of Schiff bases and their mixed ligand metal complexes derived from 4,6-diacetylresorcinol, Journal of Saudi Chemical Society 18 (2014) 190-199.

[13] N. Leopold, L, Szabó, A. Pîrnau, M. Aluas, L. F. Leopold, V. Chis, O. Cozar, Raman spectroscopic and DFT theoretical study of 4-(2-pyridylazo)resorcinol and its complexes with zinc(II) and copper(II), Journal of Molecular Structure 919 (2009) 94–99.

[14] F. Karipcin, E. Kabalcilar, S. Ilican, Y. Cağlar, M. Cağlar, Synthesized some 4-(2-thiazolylazo)resorcinol complexes: Characterization, thermal and optical properties, Spectrochimica Acta Part A: Molecular and Biomolecular Spectroscopy, Spectrochimica Acta Part A 73 (2009) 174–180.

[15] D. M. Patel, T. S. Patel, B. C. Dixit, Synthesis, characterization and dyeing performance of new bisazo–bisazomethine disperse dyes, Journal of Saudi Chemical Society 17 (2013) 203-209.

[16] R. A. Bawa, E. M. Alzaraide, Study of the Azo Hydrazone Tautomerism in the 4-(9-Anthrylazo) Phenol, World Academy of Science, Engineering and Technology, International Journal of Chemical, Molecular, Nuclear, Materials and Metallurgical Engineering 8 (3) (2014) 241-243.

[17] A. Ünal, B. Eren, E. Eren, Investigation of the azo-hydrazone tautomeric equilibrium in an azo dye involving the naphthalene moiety by UV–vis spectroscopy and quantum chemistry, Journal of Molecular Structure 1049 (2013) 303-309.

[18] J. Dostanic, D. Mijin, G. Uscumlic, D.M. Jovanovic, M. Zlatar, D. Loncarevic. Spectroscopic and quantum chemical investigations of substituent effects on the azo-

hydrazone tautomerism and acid-base properties of arylazo pyridine dyes, Spectro Chimica Acta Part A 123 (2014) 37-45.

[19] P. Ball, C. H. Nicholist, Azo hydrazone tautomerism of hydroxyazo compounds-A Review, Dyes and Pigments 3 (1982) 5-26.

[20] M. Dakiky, K. Kanan, M., Khamis, Aggregation of *o,o′*-dihyroxyazo dyes II. Interaction of 2-hydroxy-4-nitrophenylazoresorcinol in DMSO and DMF. Dyes and Pigments 41 (1999) 199-209.

[21] H. Kocaokutgen, İ. E. Gümrükçüoğlu, Synthesis and characterization of some novel azo dyes containing *tert*-butyl groups, Turkish Journal of Chemistry 19 (1995) 219-223.

[22] B. Babür, N. Seferoğlu, E. Aktan, T. Hökelek, E. Şahin, Z. Seferoğlu, Phenylazoindole dyes 3: Determination of azo-hydrazone tautomers of new phenylazoindole dyes in solution and solid state Journal of Molecular Structure 1081, 2015, 175-181

[23] A. Bayrakdar, H.H. Kart, S Elcin, H Deligoz, M Karabacak, Synthesis and DFT calculation of a novel 5, 17-di (2-antracenylazo)-25, 27-di (ethoxycarbonylmethoxy)-26, 28-dihydroxycalix [4] arene, Spectrochimica Acta Part A: Molecular and Biomolecular Spectroscopy 136 (2015) 607-617.

[24] N. A. Wazzana, O. S. Al-Qurashia, H. M. Faidallaha, DFT/ and TD-DFT/PCM calculations of molecular structure, spectroscopic characterization, NLO and NBO analyses of 4-(4-chlorophenyl) and 4-[4-(dimethylamino) phenyl]-2-oxo-1,2,5,6-etrahydrobenzo[h]quinoline-3-carbonitrile dyes, Journal of Molecular Liquids 223 (2016) 29–47.

[25] R. P. Tayade, N. Sekar, Benzimidazole-thiazole based NLO phoric styryl dyes with solid state emission – Synthesis, photophysical, hyperpolarizability and TD-DFT studies, Dyes and Pigments 128 (2016) 111–123.

[26] S. Poorhaji, M.Pordel, S. Ramezani, New heterocyclic green, blue and orange dyes from indazole: Synthesis, tautomerism, alkylation studies, spectroscopic characterization and DFT/TD-DFT calculations, Journal of Molecular Structure 1119 (2016) 151–156.

[27] A. Georgieva, E. Bubeva, D. Dimovb, D. Yanchevac, I. Zhivkovb, J. Krajčovičd, M. Valad, M. Weiterd, M. Machkovaa, Synthesis, structure, spectral properties and DFT quantum chemical calculations of 4-aminoazobenzene dyes. Effect of intramolecular hydrogen bonding on photoisomerization, Spectrochimica Acta Part A: Molecular and Biomolecular Spectroscopy 175 (2017) 76–91.

[28] F. Bassala, A. D. Laurenta, B. Le Guennicb, D. Jacquemin, Exploring the excited-states of squaraine dyes with TD-DFT, SOS-CIS(D) and ADC(2), Dyes and Pigments 138 (2017) 169–175.

[29] A. Regtia, H. B. E. Ayouchiab, M. R. Laamaria, S. E. Stiriba, H. Ananeb, M. El Haddad, Experimental and theoretical study using DFT method for the competitive adsorption of two cationic dyes from wastewaters, Applied Surface Science 390 (2016) 311–319.

[30] N. Şener, A. Bayrakdar, H. H. Kart, İ. Şener, A combined experimental and DFT investigation of disazo dye having pyrazole skeleton, Journal of Molecular Structure 1129 (2017) 222–230.

[31] H. Berber, C. Öğretir, E. Ç. S. Lekesiz, E. Ermis, Spectroscopic Determination of Acidity Constants of Some Monoazo Resorcinol Derivatives, Journal of Chemical & Engineering Data 53 (2008) 1049–1055.

[32] H. Kocaokutgen, S. Özkınalı, Characterisation and applications of some *o,o*'-dihydroxyazo dyes containing a 7-hydroxy group and their chromium complexes on nylon and wool, Dyes and Pigments 63 (2004) 83-88.

[33] P. Hohenberg, W. Kohn, Inhomogeneous electron gas, Physical Review 136 (1964) B864–B871.

[34] W. Kohn, L. Sham, Self-consistent equations including exchange and correlation effects, Physical Review 140 (1965) A1133–A1138.

[35] Gaussian 09, Revision B.01, M. J. Frisch, G. W. Trucks, H. B. Schlegel, G. E. Scuseria, M. A. Robb, J. R. Cheeseman, G. Scalmani, V. Barone, B. Mennucci, G. A. Petersson, H. Nakatsuji, M. Caricato, X. Li, H. P. Hratchian, A. F. Izmaylov, J. Bloino, G. Zheng, J. L. Sonnenberg, M. Hada, M. Ehara, K. Toyota, R. Fukuda, J. Hasegawa, M. Ishida, T. Nakajima, Y. Honda, O. Kitao, H. Nakai, T. Vreven, J. A Montgomer, J. E. Peralta, F. Ogliaro, M. Bearpark, J. J. Heyd, E. Brothers, K. N. Kudin, V. N. Staroverov, T. Keith, R. Kobayashi, J. Normand, K. Raghavachari, A. Rendell, J. C. Burant, S. S. Iyengar, J. Tomasi, M. Cossi, N. Rega, J. M. Millam, M. Klene, J. E. Knox, J. B. Cross, V. Bakken, C. Adamo, J. Jaramillo, R. Gomperts, R. E. Stratmann, O. Yazyev, A. J. Austin, R. Cammi, C. Pomelli, J. W. Ochterski, R. L. Martin, K. Morokuma, V. G. Zakrzewski, G. A. Voth, P. Salvador, J. J. Dannenberg, S. Dapprich, A. D. Daniels, O. Farkas, J. B. Foresman, J. V. Ortiz, J. Cioslowski, D. J. Fox, Gaussian, Inc., Wallingford CT, 2010.

[36] M. Gür, H. Kocaokutgen, M. Taş, Synthesis, spectral, and thermal characterisations of some azo-ester derivatives containing a 4-acryloyloxy group, Dyes and Pigments 72 (2007) 101-108.

[37] X. L. You, C. R. Lu, Z. L. Huang, D. C. Zhang, IR, ^{1}H NMR, ^{13}C NMR and X-ray structure determination of 1-(2′-chloro-4′-nitrophenylazo)-2,4-benzenediol, intramolecular proton transfer between oxygen and nitrogen atoms, π…π interaction and H-bonds, Dyes and Pigments. 63 (2004) 217-223.

[38] S. Özkınalı, Spectroscopic and thermal properties of newly mixed azocalix[4]arene ester derivatives, Dyes and Pigments. 107 (2014) 81-89.

[39] G. Makov, Chemical Hardness in Density Functional Theory, J. Phys. Chem., 99 (23) (1995) 9337–9339.

Table 3. ^{1}H NMR spectral results of compounds **1-8**

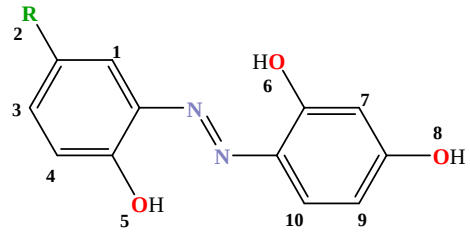

R= CH_3 (**1**), -H (**2**), -Cl (**3**), NO_2 (**4**)

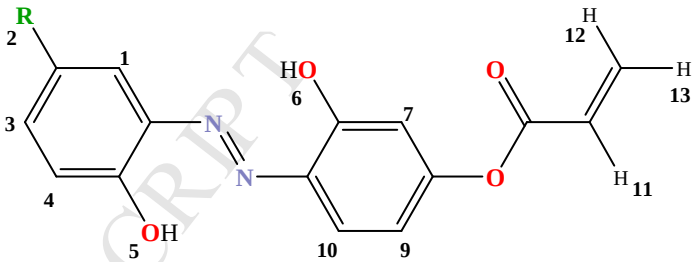

R= CH_3 (**5**), -H (**6**), -Cl (**7**), NO_2 (**8**)

Compound	OH			Azo Phenyl -H				Resorcinole-H			Acryloyl-H		
	H5	**H6**	**H8**	**H3**	**H2**	**H1**	**H4**	**H10**	**H9**	**H7**	**H12**	**H11**	**H13**
1	12.81 (s)	11.08 (s)	10.47(s)	7.68 (d) *J=7.0*	2.27 (s)	7.55 (s)	6.92 (d) *J=7.0*	7.12 (d) *J=5.5*	6.47 (d) *J=5.5*	6.37 (s)	-	-	-
2	12.68 (s)	11.42 (s)	10.49(s)	7.30 (d) *J=5.5*	6.96 (t) *J=6.5*	7.74 (d) *J=7.0*	7.69 (d) *J=6.5*	7.03 (d) *J=7.0*	6.48 (d) *J=7.0*	6.38 (s)	-	-	-
3	12.65 (s)	11.18 (s)	10.61(s)	7.72 (d) *J=7.5*	-	7.75 (s)	7.05 (d) *J=7.5*	7.31 (d) *J=8.2*	6.49 (d) *J=8.2*	6.37 (s)	-	-	-
4	12.79 (s)	12.36 (s)	10.77(s)	8.15 (d) *J=5.0*	-	8.49 (s)	6.51 (d) *J=5.0*	7.76 (d) *J=7.5*	7.21 (d) *J=7.5*	6.38 (s)	-	-	-
5	12.84 (s)	11.09 (s)	-	7.67 (d) *J=7.0*	2.27(s)	7.54 (s)	6.92 (d) *J=7.0*	7.10 (d) *J=5.5*	6.48 (d) *J=5.5*	6.33 (s)	7.35-7.16 (m)	6.58-6.50 (m)	6.22-6.17 (m)
6	12.80 (s)	11.46 (s)	-	7.29 (t) *J=6.5*	6.96 (t) *J=6.5*	7.67 (d) *J=7.5*	7.73 (d) *J=6.5*	7.88 (d) *J=7.5*	7.06 (d) *J=4.0*	6.37 (s)	6.87-6.85 (m)	6.49 (d) *J=4.0*	6.22-6.15 (m)
7	12.65 (s)	11.18 (s)	-	7.71 (d) *J=10.0*	-	7.75 (s)	7.06 (d) *J=10.0*	7.31 (d) *J=10.0*	6.93 (d) *J=10.0*	6.37 (s)	7.58-7.40 (m)	6.60-6.45 (m)	6.25-6.16 (m)
8	13.15 (s)	11.98 (s)	-	8.15-8.12 (m)	-	8.70 (s)	7.78-7.71 (m)	7.95 (d) *J=7.5*	7.60 (d) *J=7.5*	6.30 (s)	6.98-6.78 (m)	6.57-6.48 (m)	6.13-6.07 (m)

Table 4. ^{13}C NMR spectral results of compounds **1-8**

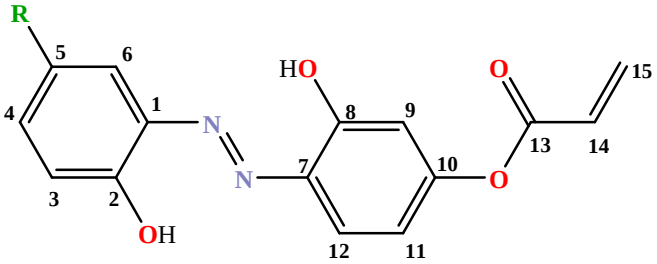

R= CH_3 (**1**,**5**), -H (**2**,**6**), -Cl (**3**,**7**), NO_2 (**4**,**8**)

Compound	C13	C10	C8	C2	C15	C4	C14	C5	C6	C12	C1	C7	C3	C11	C9	R
1	-	162.9	157.3	151.4	-	137.0	-	132.7	132.4	128.9	128.3	121.4	117.8	109.4	103.5	20.5
2	-	163.1	157.4	153.5	-	137.5	-	122.1	128.0	132.4	131.9	120.1	118.0	109.5	103.5	-
3	-	163.8	157.8	152.7	-	138.3	-	129.0	131.1	124.1	132.8	119.6	119.3	109.9	103.6	-
4	-	164.4	159.6	158.3	-	129.5	-	132.9	137.0	126.4	140.6	118.4	114.9	110.2	103.4	-
5	164.6	155.4	153.8	152.5	138.3	134.7	129.2	124.9	127.9	128.5	134.5	123.7	118.7	114.1	111.3	21.0
6	164.5	162.3	155.4	154.3	137.8	138.7	128.1	132.1	136.0	121.8	118.9	120.3	118.8	109.6	103.6	-
7	164.4	157.3	152.2	145.5	143.2	137.8	134.6	126.8	127.4	123.6	131.5	118.7	116.7	109.3	102.9	-
8	164.9	159.0	150.9	157.8	142.7	124.9	135.1	127.3	133.3	114.5	146.1	117.9	112.0	109.7	102.9	-

TABLES

Table 1. IR spectral results of compounds **1-8**
Table 2. The UV-Vis data of the compounds (1-8)
Table 3 ^{1}H NMR spectral results of compounds 1-8
Table 4 ^{13}C NMR spectral results of compounds **1-8**
Table 5. The UV-Vis data of azo forms calculated by some method and basis sets (BS1, BS2 and BS3) in solvents (S1, S2 and S3)
Table 6 Theoretical UV-Vis results for possible tautomeric structures in DMF solvent
Table 7. Theoretical calculations of molecules 1-8 (B3lyp/6-311++g(2d,2p))
Table 8. Theoretical calculations of possible hydrazone **C** and **E** (by method B3LYP with 6-311++g(2d,2p) basis set)

Table 1. IR spectral results of compounds **1-8**

Compound	ν_{O-H}	$\nu_{C-H\ Arom.}$	$\nu_{C-H\ Alkene}$	$\nu_{C=O}$	$\nu_{C=C}$	ν_{Ar-O}	Other functional groups
1	**3277**	**3067**	**-**	**-**	**1621**	**1178**	**2976 and 2916 (CH_3)**
2	**3488 3199**	**3095**	**-**	**-**	**1623**	**1167**	**-**
3	**3447 3187**	**3080**	**-**	**-**	**1627**	**1169**	**980 (C-Cl)**
4	**3492 3404**	**3093**	**-**	**-**	**1621**	**1182**	**1516 and 1338 (NO_2)**
5	**3198**	**3072**	**2922**	**1742**	**1624 1601**	**1240 1160**	**2922 (CH_3)**
6	**3202**	**3064**	**2922 2853**	**1740**	**1615 1581**	**1241 1125**	**-**
7	**3082**	**3082**	**2970 2852**	**1746**	**1622 1595**	**1256 1158**	**979 (C-Cl)**
8	**3178**	**3100**	**2918 2853**	**1749**	**1623 1578**	**1211 1112**	**1527 and 1343 (NO_2)**

Table 2. The Uv-Vis data of the related compounds (1-8)

	Wavelength [λ_{max}(nm)] (logε (L/mol.cm))				
Compound	**$CHCl_3$**	**EtOH**	**DMF**	**(pH= 1-2) (DMF)**	**(pH= 12) (DMF)**
1	435 (4.61)	400^s (4.73) 429 (4.77)	428 (4.60) 496^s (4.36)	401 (4.43)	360 (3.94) 505 (4.22)
2	400^s (4.59) 428 (4.64)	397^s (4.62) 421 (4.61)	400 (4,64) 435^s (4.59) 491^s (4.26)	396 (4.51) 431^s (4.45) 500^s (4.06)	497 (4.63)
3	408^s (4.46) 436 (4.53)	407^s (4.77) 423 (4.73)	425 (4.75) 516^s (4.29)	408 (4.59) 423^s (4.58)	497 (4.70)
4	401^s (4.75) 431 (4.83)	402 (4.74) 413^s (4.73)	415 (4.61) 510 (4.63)	404 (4.54)	450^s (4.68) 504 (4.72)
5	401^s (4.46) 430 (4.50)	399^s (4.70) 415 (4.69)	408 (4.52) 523^s (4.11)	420 (4.46) 484^s(4.12)	503 (4.58)
6	393 (4.59) 423^s (4.60)	395 (4.76) 421^s (4.72)	402 (4.56) 428^s (4.53) 490^s (4.25)	412 (4.42) 433^s (4.39) 511^s (4.02)	498 (4.58)
7	343^s(4.51) 400 (4.54) 431^s(4.58)	403 (4.79)	412 (4.57) 501^s (4.32)	407 (4.52) 431^s (4.49)	495 (4.66)
8	396 (4.82)	420 (4.54) 469^s (4.44)	392^s (4.31) 502 (4.58) 529^s (4.53)	399 (4.43) 441^s(4.37)	449^s (4.46) 510 (4.50)

^{s}: Shoulder peaks

Table 5. The UV-Vis data of azo forms calculated by some method and basis sets (BS1, BS2 and BS3) in solvents (S1, S2 and S3)

Compound	Methods and Basis Sets											
	M06/bs1			PBE1PBE/bs2			B3LYP/bs3			B3LYP/bs4		
	S1	*S2*	*S3*	*S1*	*S2*	*S3*	*S1*	*S2*	*S3*	*S1*	*S2*	*S3*
1	445	450	442	414	413	411	429	428	426	442	441	439
2	434	433	431	403	402	400	417	416	414	428	427	425
3	441	439	437	414	413	404	429	427	425	435	433	431
4	427	426	424	397	397	395	411	407	406	418	418	416
5	456	455	453	420	419	416	443	433	431	447	445	444
6	443	442	440	411	410	408	427	426	424	437	436	434
7	451	449	447	421	418	417	434	431	430	440	436	440
8	437	435	434	402	400	399	415	412	411	433	418	417

S1:*Chloroform,* **S2**:*DMF,* **S3**:*Ethanol;* **bs1**: 3-21g**, bs2**: cc-pvtz**, bs3**: 6-311++g(2d,2p)**, bs4**: 6-311++g

Table 6. Theoretical UV-Vis results for possible tautomeric structures in DMF solvent

Method and Compound		Hydrazone forms (resorcinol dyes)			Compound	Hydrazone forms (acryloyl derivatives)	
		A	B	C		D	E
M06/bs1	**1**	477	462	498	**5**	500	486
	2	464	446	490	**6**	485	487
	3	464	443	503	**7**	487	501
	4	449	424	504	**8**	476	505
B3LYP/bs3	**1**	474	465	506	**5**	493	499
	2	463	448	495	**6**	481	486
	3	467	453	513	**7**	487	505
	4	453	422	503	**8**	470	496

bs1: 3-21g**, bs3**: 6-311++g(2d,2p)

Table 7. Theoretical calculations of molecules 1-8 (B3lyp/6-311++g(2d,2p))

Molecule	*E* (au)	E_{homo} (eV)	E_{lumo} (eV)	ΔE	η (eV)	σ (eV^{-1})	χ (eV)	*m (Debye)*
1	-838.030	-5.944	-2.670	3.274	1.637	0.611	4.307	1.147
2	-798.701	-6.069	-2.722	3.347	1.674	0.598	4.396	1.671
3	-1258.324	-6.180	-2.924	3.256	1.628	0.614	4.552	3.894
4	-1003.271	-6.582	-3.198	3.384	1.692	0.591	4.890	7.840
5	-1028.819	-6.090	-2.873	3.217	1.609	0.622	4.482	1.818
6	-989.490	-6.224	-2.923	3.301	1.651	0.606	4.574	1.712
7	-1449.113	-6.320	-3.089	3.231	1.616	0.619	4.705	3.062
8	-1194.060	-6.728	-3.353	3.375	1.688	0.593	5.041	6.821

E: Energy; ΔE: $E_{lumo} - E_{homo}$; η: Chemical Hardness ; σ: Chemical softness χ: Electronegativity; ***m***: Dipole moment

Table 8. Theoretical calculations of possible hydrazone **C** and **E** (by method B3LYP with 6-311++g(2d,2p) basis set)

Molecule	E (au)	E_{homo} (eV)	E_{lumo} (eV)	ΔE	η (eV)	σ (eV^{-1})	χ (eV)	*m (Debye)*
1-C	-838.032	-5.723	-3.020	2.703	1.352	0.740	4.372	1.154
2-C	-798.703	-5.849	-3.075	2.774	1.387	0.721	4.462	2.313
3-C	-1258.326	-5.872	-3.201	2.671	1.336	0.749	4.537	5.090
4-C	-1003.280	-6.239	-3.469	2.770	1.385	0.722	4.854	12.122
5-E	-1028.823	-5.917	-3.144	2.773	1.387	0.721	4.531	2.339
6-E	-989.493	-6.058	-3.205	2.853	1.427	0.701	4.632	2.505
7-E	-1449.116	-6.070	-3.332	2.738	1.369	0.730	4.701	3.873
8-E	-1194.069	-6.469	-3.616	2.853	1.427	0.701	5.043	10.146

E: Energy; ΔE: $E_{lumo} - E_{homo}$; η: Chemical Hardness ; σ: Chemical softness ; χ: Electronegativity; m: Dipole moment

CAPTIONS

Figure 1 The synthesis of *o,o'*-dihyroxyazo dyes including acryloyl moiety

Figure 2 Dihedral scanning of the compound **1**

Figure 3. The IR spectrum for 3-Hydroxy-4-[(*E*)-(5-chloro-2-hydroxyphenyl)diazenyl]-phenyl prop-2-enoat, 6

Figure 4 The UV-Vis spectra of 3-Hydroxy-4-[(*E*)-(5-chloro-2-hydroxyphenyl)diazenyl]-phenyl prop-2-enoat (**7**), in $CHCl_3$, EtOH, DMF, DMF (pH = 2), DMF (pH = 12) 1.0 $x10^{-5}$ $mol.L^{-1}$.

Figure 5 The Azo-Hydrazone tautomer forms of the compounds

Figure 6 The ^{1}H-NMR spectrum for 3-Hydroxy-4-[(*E*)-(5-chloro-2-hydroxyphenyl)diazenyl]-phenyl prop-2-enoat, 6

Figure 7 HOMO-LUMO and ESP maps of compounds **1** and **2**, and their tautomeric forms (**C** and **E**).

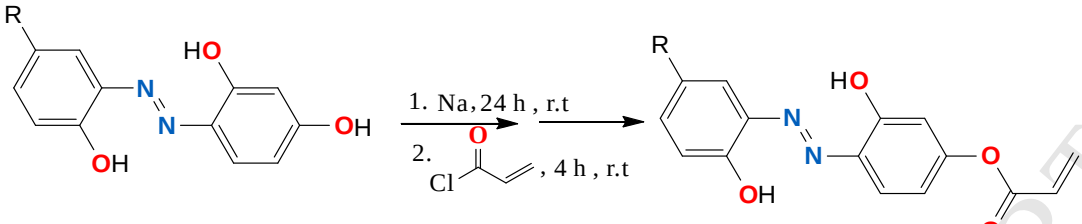

1 R= -CH_3
2 R= -H
3 R= -Cl
4 R= -NO_2

5 R= -CH_3
6 R= -H
7 R= -Cl
8 R= -NO_2

Figure 1. The synthesis of *o,o'*-dihyroxyazo dyes including acryloyl moiety

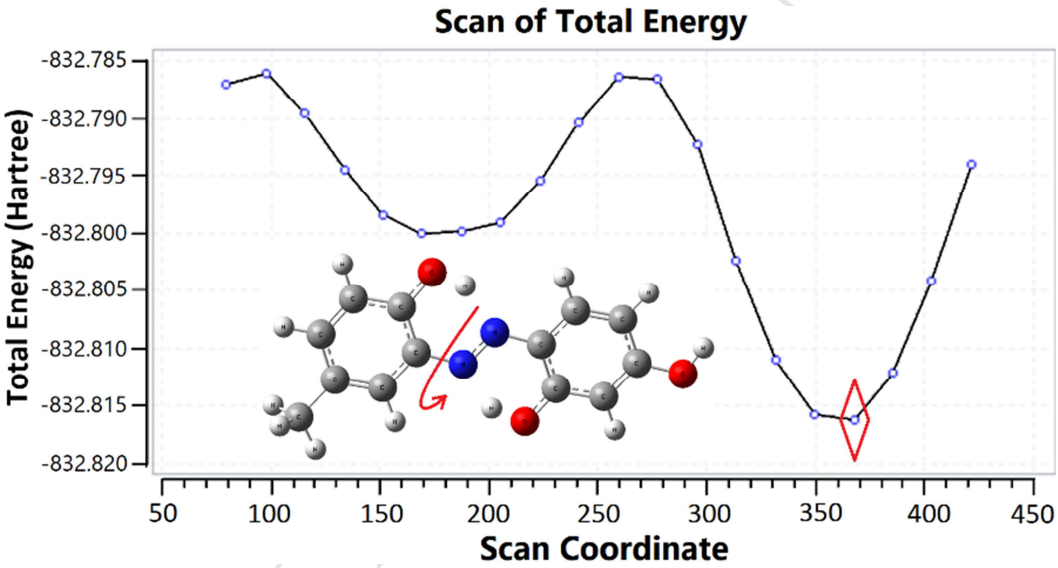

Figure 2. Dihedral scanning of the compound **1**

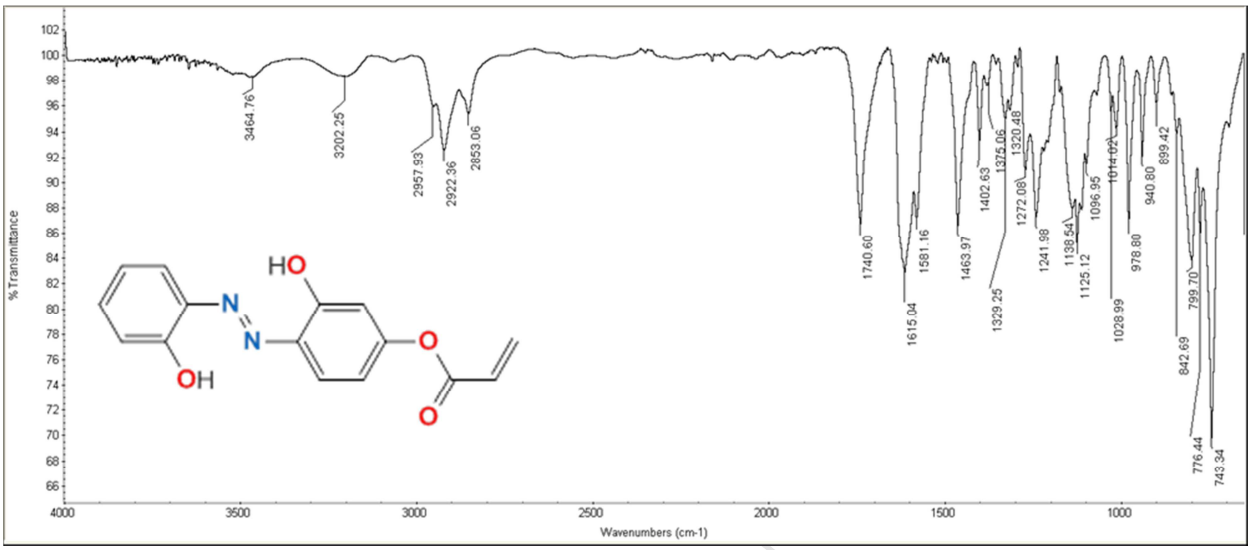

Figure 3. The IR spectrum for 3-Hydroxy-4-[(*E*)-(5-chloro-2-hydroxyphenyl)diazenyl]-phenyl prop-2-enoat, 6

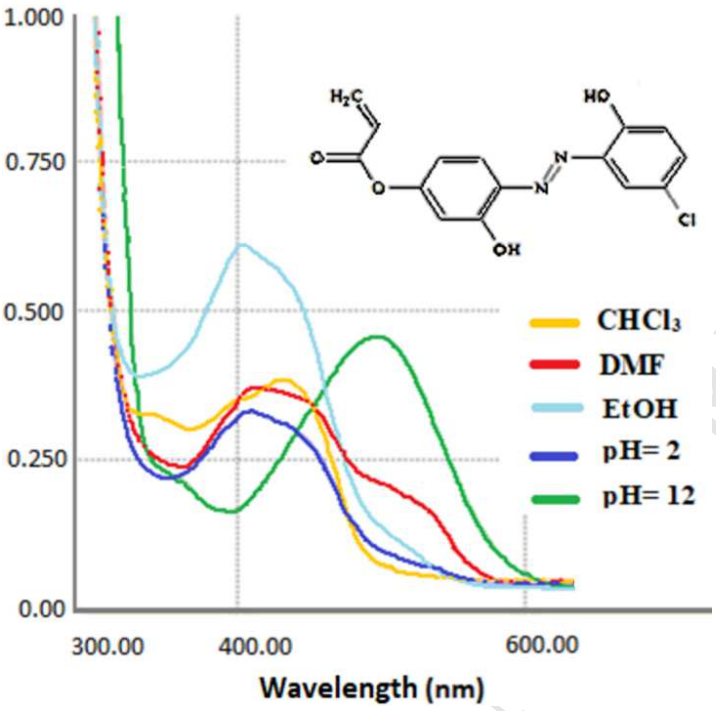

Figure 4. The UV-Vis spectra of 3-Hydroxy-4-[(*E*)-(5-chloro-2-hydroxyphenyl)diazenyl]phenyl prop-2-enoat (**7**), in $CHCl_3$, EtOH, DMF, DMF (pH = 2), DMF (pH = 12) 1.0 $x10^{-5}$ $mol.L^{-1}$.

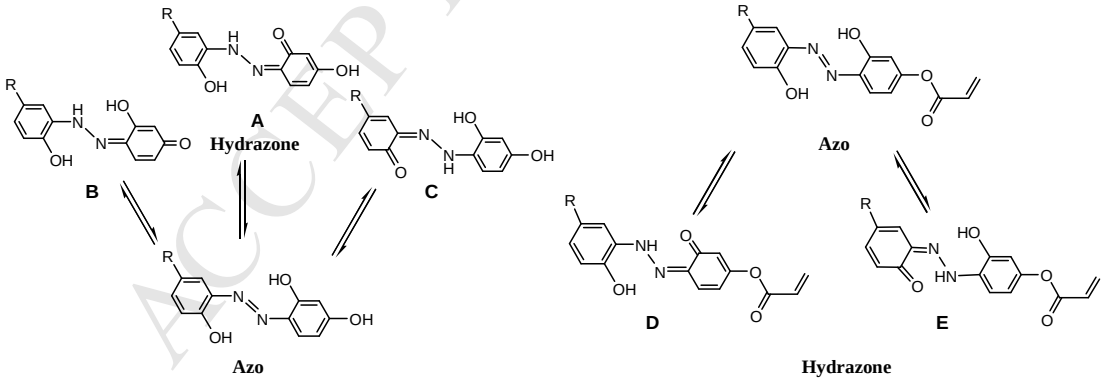

Figure 5. The Azo-Hydrazone tautomer forms of the compounds

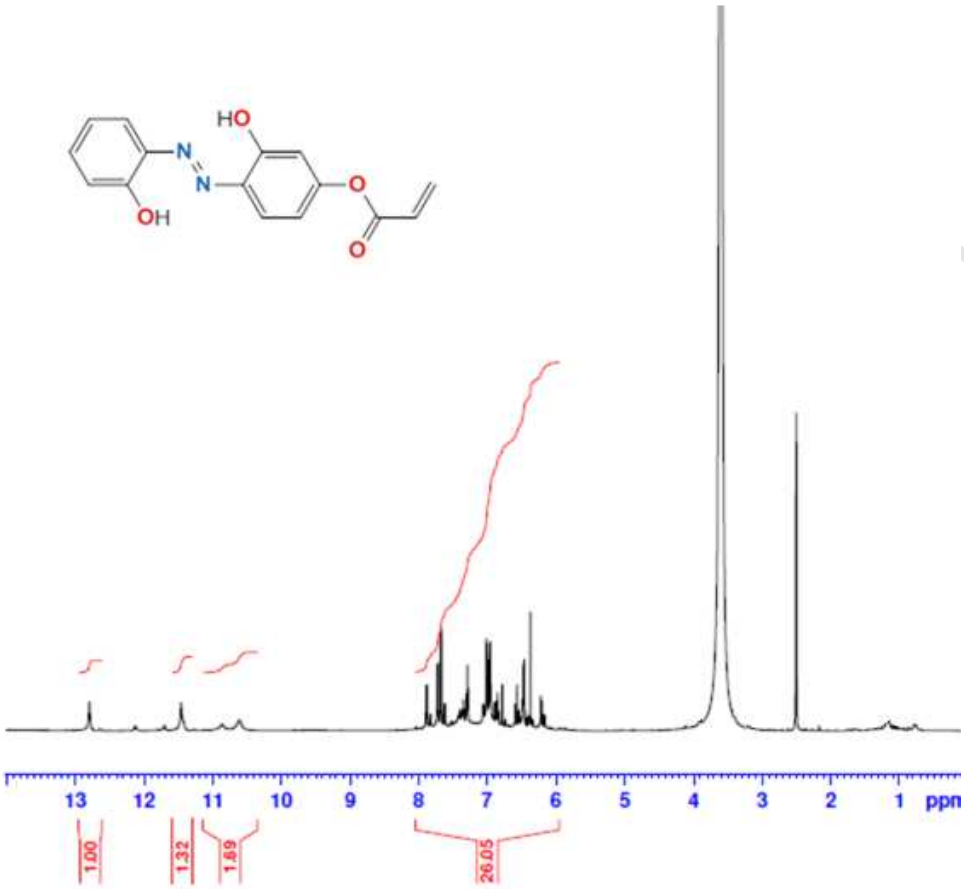

Figure 6. The ^{1}H-NMR spectrum for 3-Hydroxy-4-[(*E*)-(5-chloro-2-hydroxyphenyl)diazenyl]-phenyl prop-2-enoat, 6

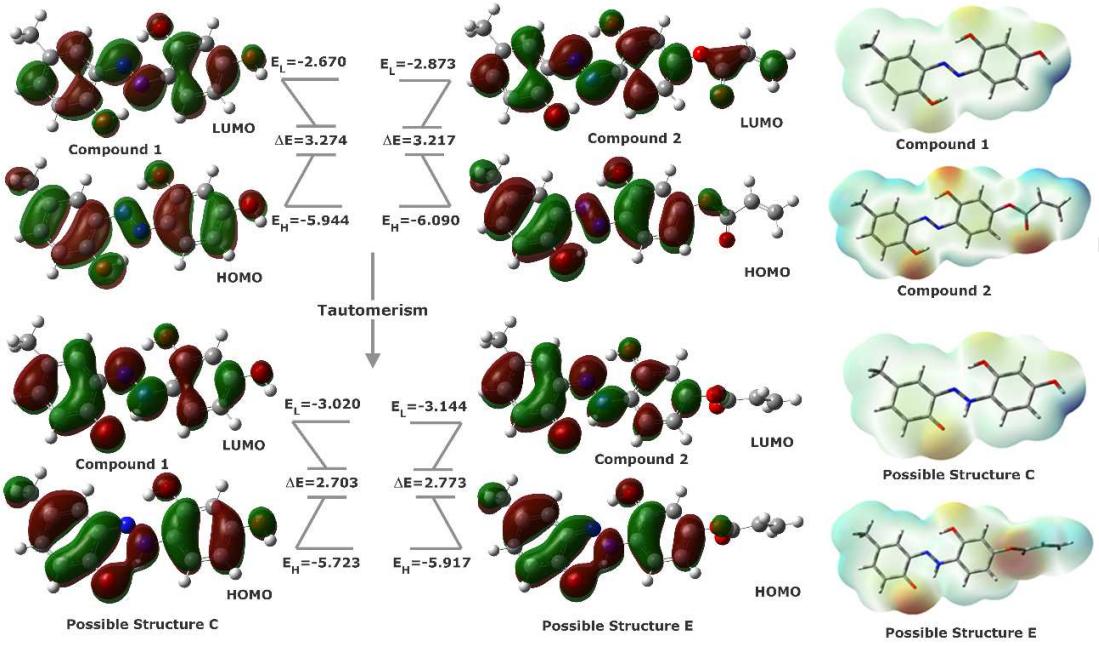

Figure 7. HOMO-LUMO and ESP maps of compounds **1** and **5**, and their tautomeric forms (**C** and **E**).

SCHEME

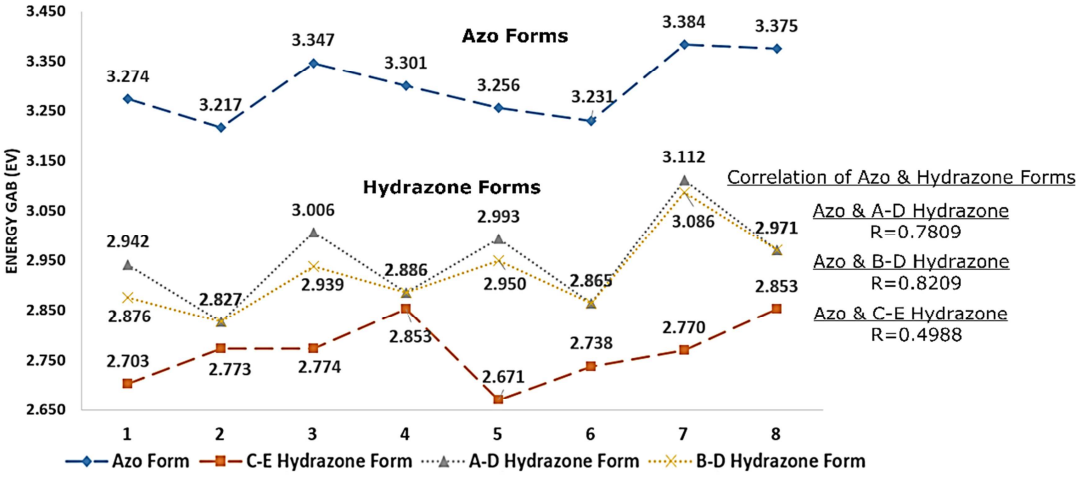

Graphic 1. Energy gab (ΔE) of possible hydrazone forms, and correlation with azo forms

Highlights

- Novel *o*,*o*'-dihydroxyazo dyes containing an acryloyl moiety were synthesized and characterized.
- The azo–hydrazone tautomerism was investigated using UV–Vis spectroscopy and DFT calculations.
- These compounds are useful for synthesizing novel organic dyes.